NANO LETTERS

2008
Vol. 8, No. 9
3035-3040

Flexible Piezotronic Strain Sensor

Jun Zhou,[†,‡] Yudong Gu,[†,§] Peng Fei,[†,§] Wenjie Mai,[†] Yifan Gao,[†] Rusen Yang,[†] Gang Bao,[‡] and Zhong Lin Wang*[,†]

School of Materials Science and Engineering, Georgia Institute of Technology, Atlanta, Georgia 30332, Department of Biomedical Engineering, Georgia Institute of Technology and Emory University, Atlanta, Georgia 30332, and Department of Advanced Materials and Nanotechnology, College of Engineering, Peking University, 100084 Beijing, China

Received August 4, 2008

ABSTRACT

Strain sensors based on individual ZnO piezoelectric fine-wires (PFWs; nanowires, microwires) have been fabricated by a simple, reliable, and cost-effective technique. The electromechanical sensor device consists of a single electrically connected PFW that is placed on the outer surface of a flexible polystyrene (PS) substrate and bonded at its two ends. The entire device is fully packaged by a polydimethylsiloxane (PDMS) thin layer. The PFW has Schottky contacts at its two ends but with distinctly different barrier heights. The *I*−*V* characteristic is highly sensitive to strain mainly due to the change in Schottky barrier height (SBH), which scales linear with strain. The change in SBH is suggested owing to the strain induced band structure change and piezoelectric effect. The experimental data can be well-described by the thermionic emission−diffusion model. A gauge factor of as high as 1250 has been demonstrated, which is 25% higher than the best gauge factor demonstrated for carbon nanotubes. The strain sensor developed here has applications in strain and stress measurements in cell biology, biomedical sciences, MEMS devices, structure monitoring, and more.

ZnO, a direct wide band gap (3.37 eV) semiconductor and one of the most important functional materials, has attracted a wide range of interest in science and technology. Quasi-one-dimensional ZnO nanostructures such as nanowires (NWs) and nanobelts (NBs)[1] are considered as important building blocks for fabricating various nanodevices. By using the unique electronic, optical, mechanical, and piezoelectric properties, ZnO NWs/NBs based field effect transistors,[2] ultraviolet (UV) lasers,[3] UV photo detectors,[4] light-emitting diodes,[5] solar cells,[6] piezoelectric transducer, and actuator[7] have been demonstrated. Most importantly, by utilizing semiconducting-piezoelectric coupled properties of ZnO, nanogenerators,[8,9] piezoelectric field effect transistors,[10] and piezoelectric diodes[11] and piezoelectric chemical sensors[12] were invented, which are the fundamental components of piezotronics.[13]

Recently, research in the field of micro- and nanoelectromechanical system (MEMS and NEMS) is rapidly growing with considerable potential for ultra fast, high-sensitivity and low-power consumption devices. As for nano- and microscale strain/stress and pressure measurements, various sensors have been fabricated based on NWs[14,15] and carbon nanotubes (CNTs).[16−19] Commonly, these devices utilize the piezoresistance property of the material, that is, under small strain, the conductance of the material changes with strain following a linear relationship.[14] CNT is the most intensively studied material in this area, and sensor device based on CNTs with gauge factor up to 850 have been achieved.[19] However, studies have shown that the piezoresistance property depends on the electronic structure of CNTs,[19] which can be metallic or semiconducting depending on their structures.

In this paper, we present the fabrication and application of an alternative design of a fully packaged strain sensor device based on a single ZnO piezoelectric fine wire (PFW; nanowire, microwire). The strain sensor was fabricated by bonding a ZnO PFW laterally on a polystyrene (PS) substrate. The *I*−*V* behavior of the device was modulated by strain due to the change in Schottky barrier height (SBH). The combined effects from strain induced band structure change and piezoelectricity result in the change of SBH. The working principle of the new type strain sensor has been presented in comparison to the theoretical model.

The schematic of the strain sensor device is shown in Figure 1a. Ultralong ZnO PFWs were synthesized by a high temperature thermal evaporation process,[1] and they typically have diameters of 2−6 μm and lengths of several hundred micrometers to several millimeters. We chose large size wires for easy manipulation under optical microscope. The same principle and methodology applies to nanowires. The typical

* Corresponding author. E-mail: zlwang@gatech.edu.
† School of Materials Science and Engineering, Georgia Institute of Technology.
‡ Department of Biomedical of Engineering, Georgia Institute of Technology and Emory University.
§ Peking University.

10.1021/nl802367t CCC: $40.75
Published on Web 08/16/2008

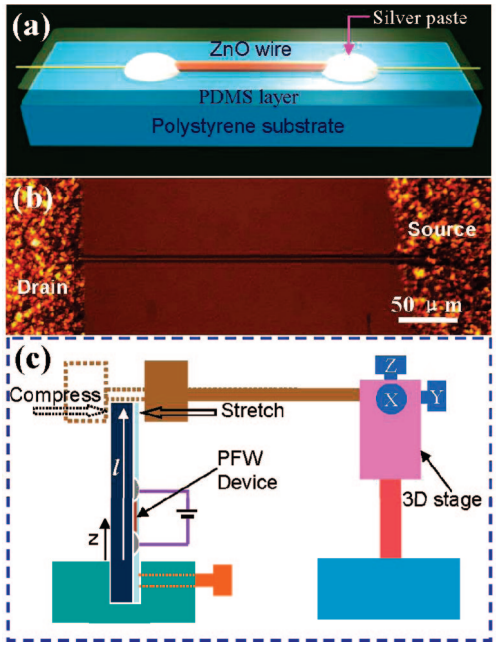

Figure 1. (a) Schematic of a single ZnO PFW based strain sensor device. (b) Optical image of a strain sensor device. (c) Schematic of the measurement system to characterize the performance of the sensor device.

PS substrate has a length of ~3 cm, width of ~5 mm, and thickness of 1 mm. The substrate was washed with deionized water and ethanol under sonication. After drying with flowing nitrogen gas and placing in a furnace at 80 °C for 30 min, the PS substrate was ready to be used as the substrate. ZnO PFW was placed on the PS substrate by using a probe station under optical microscopy. Silver paste was applied at both ends of the ZnO PFW to fix its two ends tightly on the substrate, silver paste was also used as source and drain electrodes. A thin layer of polydimethylsiloxane (PDMS) was used to package the device. The thickness of the PDMS layer is much thinner than the thickness of the PS substrate. The PDMS thin layer not only enhances the adhesion of the silver paste to the PS substrate, but also prevents the ZnO wire from contamination or corrosion. Then, the entire device was annealing at 80 °C for 12 h. Finally, a flexible, optically transparent, and well-packaged strain sensor device was fabricated. Figure 1b shows an optical image of the strain sensor device, indicating that a smooth ZnO wire was placed on the substrate with two ends fixed.

The characterization of the $I-V$ behavior of the sensor device with strain was carried out in atmosphere at room temperature, and the measuring system is schematically shown in Figure 1c. One end of the device was affixed on a sample holder that was fixed tightly on an optical air table, with another end free to be bent. An x-y-z mechanical stage with movement resolution of 1 μm was used to bend the free end of the sensor device to produce a compressive or tensile strain. Meanwhile, continuous triangle sweeping voltage was applied through the ZnO wire to measure its $I-V$ characteristics during deformation. To study the stability and response of the sensor devices, a resonator with controlled frequency and amplitude was used to periodically bend the sensor device. At the same time, a fixed bias voltage was applied between the source and the drain.

Since the thin PDMS layer has a much smaller Young's modulus (E = 360−870 KPa) than that of PS substrate (E = 3−3.5 GPa) and the silver paste electrodes have a much smaller area and thickness in comparison with those of the PS substrate, the PDMS layer and silver paste electrodes, which are bonded on the outer surface of the PS substrate, do not alter the mechanical properties of the PS film at any significant level. Therefore, the strain in the PFW is either purely tensile or compressive depending on the bending direction of the PS substrate. The strain in the PFW is approximately equal to the strain of the site z where it was placed on the outer surface of the PS substrate. With consideration of the extremely small diameter of the PFW in comparison with the thickness of the PS substrate, the axial strain ε_{zz} along the length of the PFW is approximately[20−22]

$$\varepsilon_{zz} = 3\frac{a}{l}\frac{D_{\max}}{l}\left(1-\frac{z}{l}\right) \quad (1)$$

where z is the vertical distance measured from the fixed end of the PS substrate to the middle of the PFW; a is the half-thickness of the PS substrate; l is the length of PS film from the fixed end to the free end; and D_{max} is the maximum deformation of the free end of the PS substrate, which has a negative or positive sign depending upon whether the PFW is under compressive or tensile strain, respectively. Equation

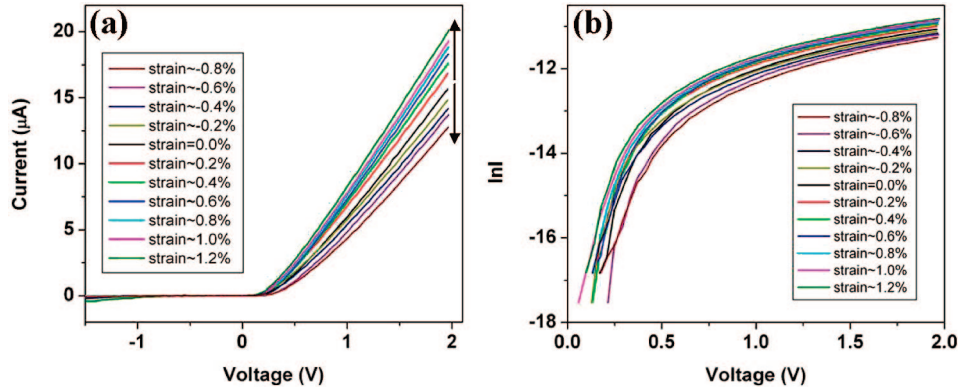

Figure 2. (a) Typical $I-V$ characteristics of the sensor at different strain. (b) Logarithm plot of the current under positive bias by using the data in (a).

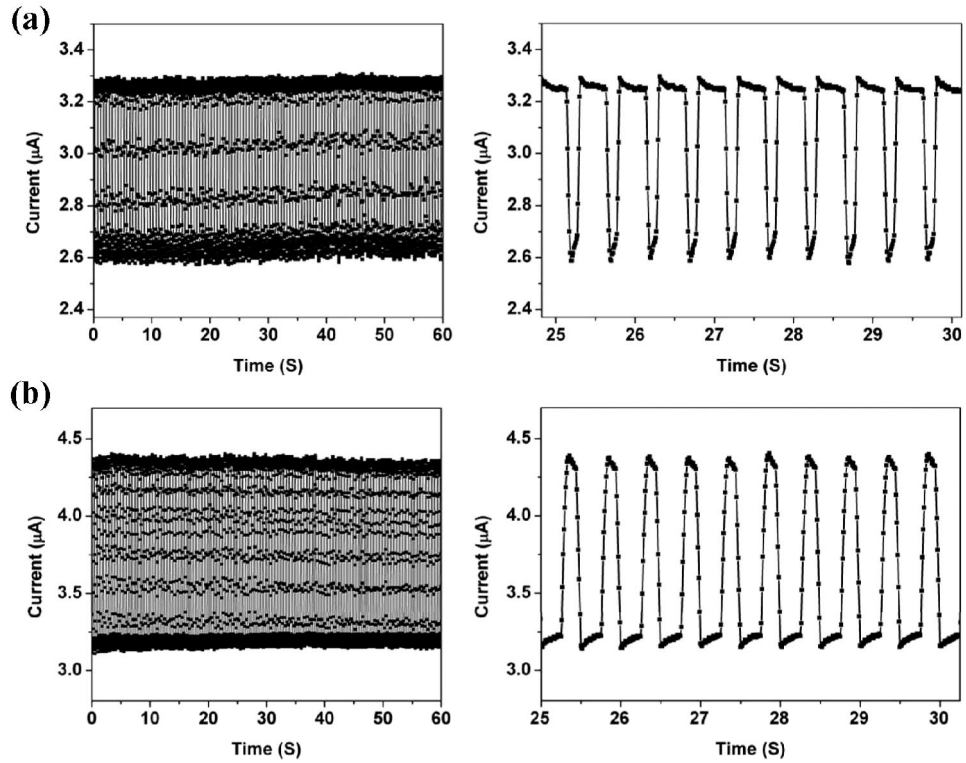

Figure 3. Current response of a sensor device that was repeatedly compressed (a) and stretched (b) at a frequency of 2 Hz under fixed bias of 2 V.

1 indicates that the strain ε_{zz} has a linear relationship with the maximum deformation D_{max}. In practice, since the length of the substrate is much larger than the length of the PFW ($l \gg L$), the strain in the PFW is uniform to an excellent approximation.

Before the electromechanical measurements, we have first measured the original $I-V$ characteristic of the sensor device. We found various $I-V$ characteristics for over 250 devices. The nonlinear $I-V$ characteristics are commonly observed in measuring semiconductor devices.[23,24] Generally, the nonlinearity is caused by the Schottky barriers formed between the semiconductor and the metal electrodes in the semiconductor device, and the shape of the $I-V$ curve depends on the heights of the Schottky barriers formed at the source and drain due to different interface properties.[24,25] In this study, we only focused on the devices that have Schottky contacts at the two ends of the PFW, but with distinctly different barrier heights. The $I-V$ curve shape is quite asymmetric. Typical $I-V$ characteristics under various strains (device #1) are shown in Figure 2a. The $I-V$ curves shift upward with tension strain and downward with compressive strain. The $I-V$ curve fully recovered when the strain was relieved.

The stability and response of the sensor device (device #2) was carefully studied. Figure 3a,b shows the current response of the sensor over many cycles of repeatedly compressing and stretching at a frequency of 2 Hz under fixed bias of 2 V, respectively. It can be seen that the current decreases with compressive strain and increases with tensile strain, which is consistent with the phenomenon observed in Figure 2a. It should be noticed that the current reached almost the same value in each cycle of straining, and the current can fully recover when the strain was relieved, indicating the sensor device had high reproducibility and good stability. Current response of the sensor device which was repeatedly stretched at frequencies of 2, 3, 5, and 10 Hz (constant amplitude under fixed bias of 2 V) was also investigated (see Supporting Information, Figure S1). A response time of ~10 ms of the sensor device can be derived.

The $I-V$ curve shown in Figure 2a clearly demonstrates that there were Schottky barriers present at the contacts but with distinctly different barrier heights. The presence of a Schottky barrier at the metal/semiconductor interface[26] plays a crucial role in determining the electrical transport property of the metal−semiconductor−metal (M-S-M) structure. By simply looking at the $I-V$ curve, one is unable to identify the nature of the barriers either reversely biased or forward biased. It is important to quantitatively simulate the shape of the $I-V$ curve in order to determine the nature of the electric transport across the M-S-M structure.[23,24] After carefully studying the shape of the $I-V$ curve, our device is considered as a single ZnO wire sandwiched between two opposite Schottky barriers, as shown in Figure 4a. We assume that the barrier height at the drain side ϕ_d (eV) is significantly higher than that at the source side. At a fixed bias voltage V, the voltage drop occurs mainly at the reversely biased Schottky barrier according to the measurement by in situ scanning surface potential microscopy.[27] In our case, when a relatively large positive voltage V is applied across the drain and source with the drain positive, the voltage drop occurs mainly at the reversely biased Schottky

barrier ϕ_s (eV) at the source side, and it is denoted by V_s. Here, we assume $V_s \approx V$. With consideration that our measurements were made at room temperature and the ZnO PFW had a low doping, the dominant transport property at the barrier is thermionic emission and diffusion, while the contribution made by tunneling can be ignored. Thus, as inspired by the shape of the ln $I-V$ curve in Figure 2b and according to the classic thermionic emission−diffusion theory (for $V \gg 3kT/q \sim 77$ mV) for a reversal bias voltage V and at temperature T, the current through the reversely biased Schottky barrier ϕ_s is given by[26]

$$I = SA^{**}T^2 \exp\left(-\frac{\phi_s}{kT}\right) \exp\left(\frac{\sqrt[4]{q^7 N_D (V + V_{bi} - kT/q)/(8\pi^2 \varepsilon_s^3)}}{kT}\right) \quad (2)$$

where S is the area of the source Schottky barrier, A^{**} is the effective Richardson constant, q is the electron charge, k is the Bolzman constant, N_D is the donor impurity density, V_{bi} is the build in potential at the barrier, and ε_s is the permittivity of ZnO. The ln $I-V$ curve shown in Figure 4b qualitative indicates that variation of ln I can be described by $V^{1/4}$ for reversely biased Schottky barrier instead of ln $I \sim V$ as for forward biased Schottky barrier. Therefore, eq 2 can be used to precisely fit the experimentally observed ln $I-V$ curve, from which the corresponding parameters can be derived. This indicates that the thermionic emission−diffusion model not only is the dominant process in our device but also can be applied to derive the SBH as described in what follows.

By assuming that S, A^{**}, T, N_D are independent of strain for small deformation,[28,29] ϕ_s can, in principle, be derived from the logarithm of the current (ln $I-V$) plot, which is shown in Figure 4b. Subsequently, the change of SBH can be determine by

$$\ln[I(\varepsilon_{zz})/I(0)] = -\Delta\phi_s/kT \quad (3)$$

where $I(\varepsilon_{zz})$ and $I(0)$ are the current measured through the PFW at a fixed bias with and without being strained, respectively. The results are plotted in Figure 4c for two biases of 1.5 and 2 V, indicating that the change of SBH $\Delta\phi_s$ has an approximately linear relationship with strain, which is consistent with the previous reports.[28,30−32] We also notice that the $\Delta\phi_s$ is not very sensitive to the choice of bias voltage V.

In the calculation presented above, we assumed that the applied voltage was totally consumed at the reversely biased Schottky barrier formed at the source electrode. In reality, $V_s < V$; thus, the calculated $\Delta\phi_s$ value may be slightly affected by the choice of V, but the linear dependence of $\Delta\phi_s$ on strain will not be affected much. Figure 4d shows the change of ln I at fixed bias of $V = 1.5$ and 2.0 V as a function of strain (device #1). The change of ln I varies approximately linear with the applied strain.

It has been reported that the SBHs of GaAs,[30,31] GaN,[32] and GaAlN[33] Schottky barrier shift under stress and strain due to the band structure change and piezoelectric effect. Experiments and calculations have shown that the band gap

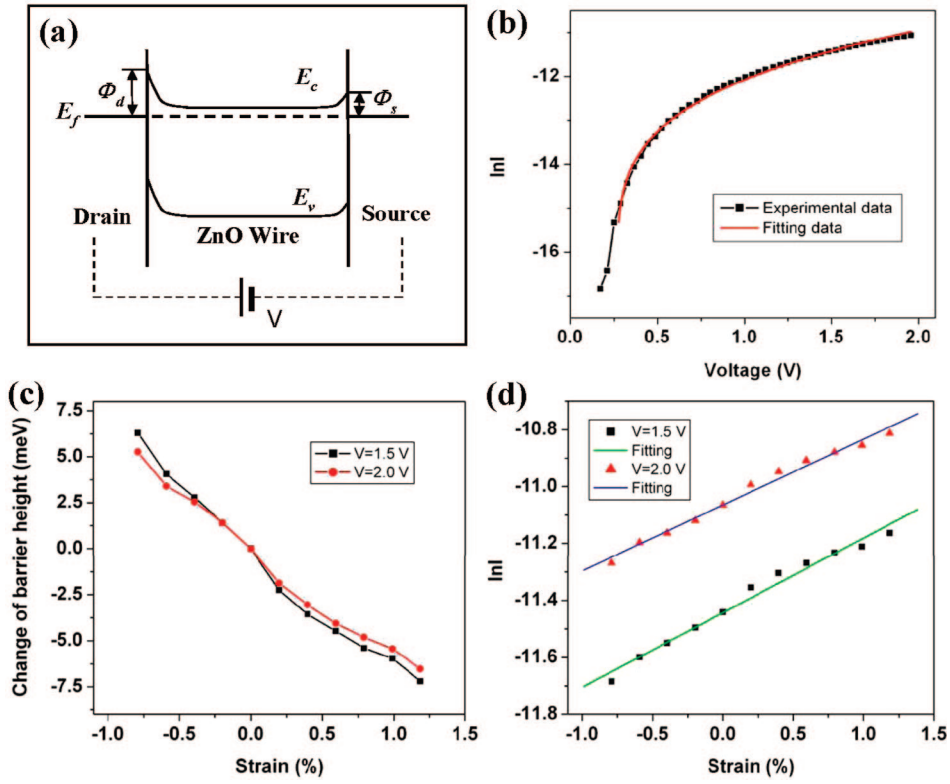

Figure 4. (a) Energy band diagram illustrates the asymmetric Schottky barrier heights at the source and drain contacts of a PFW, where the offset by the applied drain-source voltage V was not included for easy discussion. (b) Fitting the ln $I-V$ data using the thermionic emission−diffusion theory at a given strain for a reversely biased Schottky barrier. The black dotted lines are experimental data points from Figure 2b for strain = 0, and the red line is the theoretical fit. (c) The derived change in SBH based on the thermionic emission−diffusion model, as a function of stain at a drain-source bias of $V = 1.5$ and 2.0 V, respectively. (d) Logarithm plot of the current (in unit of ampere) at fixed bias of $V = 1.5$ and 2.0 V as a function of strain.

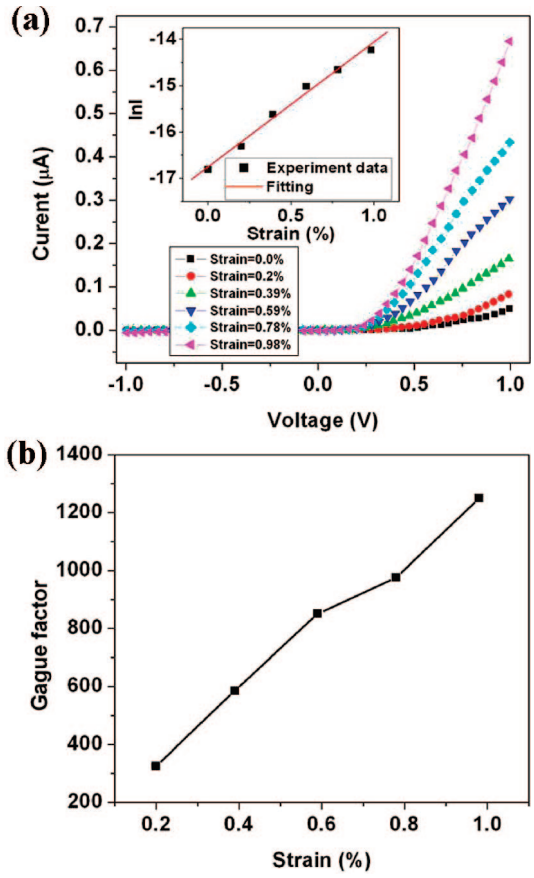

Figure 5. (a) $I-V$ characteristics of device #3 under different strain. Inset is the dependence of ln I (in unit of ampere) on the applied strain. (b) Gauge factors derived from (a) as a function of strain.

changes under strain and stress.[33,34] Similarly, the SBH change for ZnO under strain can be viewed as a combination of band structure change and piezoelectric effects. In using a simple Schottky model, the effect of the band structure change may be equivalently characterized by a change in semiconductor (ZnO) electron affinity under strain, which is denoted as $\Delta\phi_{s-bs}$.

The effect of piezoelectric polarization on the SBH arises because the polarization produces surface charges at an interface where the divergence of the polarization is nonzero, that is, at the metal−semiconductor interface and beneath the depletion region in the semiconductor.[31] At the later position, the associated polarization charge may be screened by the conduction electrons. On the other hand, at the metal−semiconductor interface, the polarization charge can be partially neutralized by an adjustment of the electronic charges in the interface states or in the metal.[31] This effect will shift the Fermi level at the interface and subsequently affects the SBH. The change in SBH by piezoelectric polarization is given approximately by[31]

$$\Delta\phi_{s-pz} = \frac{\sigma_{pz}}{D}\left(1+\frac{1}{2q_s d}\right)^{-1} \quad (4)$$

Here, σ_{pz} is the area density of piezoelectric polarization changes (in units of electron charge), D is a two-dimensional density of interface states at the Fermi level in the semiconductor band gap at the Schottky barrier, and d is the width of the depletion layer. Associated with the states in the band gap at interface is a two-dimensional screening parameter $q_s = (2\pi q^2/k_0)D$, where q is the electronic charge and k_0 is the dielectric constant of the ZnO. Thus, the total change in SBH of ZnO sensor can be expressed as

$$\Delta\phi_s = \Delta\phi_{s-bs} + \Delta\phi_{s-pz} \quad (5)$$

In this study, $\Delta\phi_s$ decreases under tension strain and increases under compressive strain, and the experimentally observed strain effect is a combined result of $\Delta\phi_{s-bs}$ and $\Delta\phi_{s-pz}$. Experimentally, the contribution made by band structure change is stationary as long as the strain is preserved, while the contribution from piezoelectric effect could be time dependent with a slight decay (Supporting Information, Figure S2), possibly because of charge trapping effect by impurity and vacancy states in ZnO, which may result in a slow change in conductivity, similar to the slow recovery of the ZnO conductivity after illumination by UV light. Further study is required to fully understand this phenomenon.

For practical application, the performance of a strain sensor is characterized by a gauge factor, which is defined to be the slope of the normalized current (I)−strain (ε) curve, $[\Delta I(\varepsilon)/I(0)]/\Delta\varepsilon$. The highest gauge factor demonstrated for our sensor device is 1250 (Figure 5b; device #3), which exceeds the gauge factor of conventional metal strain gauges (1−5) and state-of-the-art doped-Si strain sensor (∼200), and even higher than the highest gauge factor reported for CNTs (∼1000).[35] Figure 5a shows the $I-V$ curve of another device (device #3) as a function of the applied strain, which shows the same behavior as that presented in Figure 2a. The inset indicates that ln I linearly depends on the applied strain. The gauge factor determined as a function of the strain is presented in Figure 5b, and it is consistent with the calculated results.[36]

In practice, some of the devices showed relatively low gauge factor, which may be attributed to the opposite signs of $\Delta\phi_{s-bs}$ and $\Delta\phi_{s-pz}$ because the piezoelectric effect depends on the orientation of the c axis of the ZnO wire.[8] We had 50% chance in experiments to have the ZnO wire oriented along the c or $-c$ direction.

In summary, a new type fully packaged strain sensor device based on a single ZnO PFW has been demonstrated. The strain sensor was fabricated by bonding a ZnO PFW laterally on a flexible PS substrate and was packaged by a PDMS thin film. The sensor devices have excellent stability, fast response, and high gauge factor of up to 1250. The $I-V$ characterization of the device is modulated by the change of SBH, which has a linear relationship with strain. The underlying mechanism for the change of SBH was attributed to the combination of strain induced band structure change and piezoelectric effect. A combination of semiconductor and piezoelectric effects in this device is the piezotronic effect.[13] The strain sensor developed here based on a flexible substrate has application in strain and stress measurements in cell biology, biomedical sciences, MEMS devices, structure monitoring, and even earthquake monitoring.

Acknowledgment. This research was supported by DARPA, BES DOE, NSF, and Emory-Georgia Tech CCNE

funded by NIH. P.F. and Y.D.G. thank the partial fellowship support by the China Scholarship Council (CSC) (No. 20073020).

Supporting Information Available: Current response and time dependent decay data. This material is available free of charge via the Internet at http://pubs.acs.org.

References

(1) Pan, Z. W.; Dai, Z. R.; Wang, Z. L. *Science* **2001**, *291*, 1947.
(2) Arnold, M.; Avouris, P.; Pan, Z. W.; Wang, Z. L. *J. Phys. Chem. B* **2003**, *107*, 659.
(3) Huang, M.; Mao, S.; Feick, H.; Yan, H.; Wu, Y.; Kind, H.; Weber, E.; Russo, R.; Yang, P. *Science* **2001**, *292*, 1897.
(4) Soci, C.; Zhang, A.; Xiang, B.; Dayeh, S. A.; Aplin, D. P. R.; Park, J.; Bao, X. Y.; Lo, Y. H.; Wang, D. *Nano Lett.* **2007**, *7*, 1003.
(5) Park, W. I.; Yi, G. C. *Adv. Mater.* **2004**, *16*, 87.
(6) Law, M.; Greene, L. E.; Johnson, J. C.; Saykally, R.; Yang, P. D. *Nat. Mater.* **2005**, *4*, 455.
(7) Buchine, B. A.; Hughes, W. L.; Degertekin, F. L.; Wang, Z. L. *Nano Lett.* **2006**, *6*, 1155.
(8) Wang, Z. L.; Song, J. H. *Science* **2006**, *312*, 242.
(9) Wang, X. D.; Song, J. H.; Liu, J.; Wang, Z. L. *Science* **2007**, *316*, 102.
(10) Wang, X. D.; Zhou, J.; Song, J. H.; Liu, J.; Xu, N. S.; Wang, Z. L. *Nano Lett.* **2006**, *6*, 2768.
(11) He, J. H.; Hsin, C. L.; Liu, J.; Chen, L. J.; Wang, Z. L. *Adv. Mater.* **2007**, *19*, 781.
(12) Lao, C. S.; Kuang, Q.; Wang, Z. L.; Park, C. M.; Deng, Y. *Appl. Phys. Lett.* **2007**, *90*, 262107.
(13) Wang, Z. L. *Adv. Mater.* **2007**, *19*, 889.
(14) Toriyama, T.; Funai, D.; Sugiyama, S. J. *Appl. Phys. Lett.* **2003**, *93*, 561.
(15) He, R. R.; Yang, P. D. *Nat. Nanotech.* **2006**, *1*, 42.
(16) Tombler, T. W.; Zhou, C. W.; Alexseyev, L.; Kong, J.; Dai, H. J.; Liu, L.; Jayanthi, C. S.; Tang, M. J.; Wu, S. *Y Nature* **2000**, *405*, 769.
(17) Stampfer, C.; Helbling, T.; Obergfell, D.; SchÖberle, B.; Tripp, M. K.; Jungen, A.; Roth, S.; Bright, V. M.; Hierold, C. *Nano Lett.* **2006**, *6*, 233.
(18) Chang, N. K.; Su, C. C.; Chang, S. H. *Appl. Phys. Lett.* **2008**, *92*, 063501.
(19) Grow, R. J.; Wang, Q.; Cao, J.; Wang, D. W.; Dai, H. J. *Appl. Phys. Lett.* **2005**, *86*, 093104.
(20) Soutas-Little, R. W. *Elasticity, XVI, 431*; Dover Publications: Mineola, NY, 1999.
(21) Landau, L. D.; Lifshiëtìs, E. M. *Theory of elasticity*; Reading, Mass., Pergamon Press, and Addison-Wesley Pub. Co.: London, 1959.
(22) Because of the small size of the ZnO wire, the mechanical behavior of the plastic substrate is not affected by the ZnO wire. As a simple estimation of the strain, we use the Saint-Venant bending theory for small deflections.[20] The shape of the plastic substrate can be approximated as a beam, with the thickness $2a$, width w and length l. Let us establish the coordinate system so that the origin is at the center of the cross section of the fixed side, while the z axis is parallel to the length l and x axis is parallel to the width w. To calculate how the nanowire elongates or shortens as the substrate is deflected under an external bending force f_y, we only need to calculate the ε_{zz}component of the strain, so that $\varepsilon_{zz} = \Delta L_{wire}/L_{wire}$. On the other hand,[20] $\sigma_{zz} = -f_y/I_{xx}y(l-z)$,$\sigma_{xx} = \sigma_{yy} = 0$, where I_{xx} is the geometrical moment of inertia for the beam cross section. Therefore, $\Delta L_{wire}/L_{wire} = \varepsilon_{zz} = \sigma_{zz}/E$. The lateral deflection D_{max} of the pushed end is experimentally easier to measure than the bending force f_y. The relationship between D_{max} and f_y is[21] $D_{max} = f_y l^3/3EI_{xx}$ Therefore, $\varepsilon_{zz} = -3y/lD_{max}/l(1-z/l)$ The nanowire is attached at $y = \pm a$ and $z = z_0$, where z_0 is the distance from the fixed end to the nanowire. Here, the positive and negative sign for y stand for the right (compressed) side and left (tensile) side of the nanowire, respectively. Therefore,

$$\frac{\Delta L_{wire}}{L_{wire}} = \mp 3\frac{a}{l}\frac{D_{max}}{l}\left(1-\frac{z_0}{l}\right) \quad (1)$$

As expected, this strain value is dimensionless and eq 1 does not include the Young's modulus E. The negative value stands for the compressed side, and the positive value stands for the tensile side.
(23) Zhang, Z. Y.; Jin, C. H.; Liang, X. L.; Chen, Q.; Peng, L. M. *Appl. Phys. Lett.* **2006**, *88*, 073102.
(24) Zhang, Z. Y.; Yao, K.; Liu, Y.; Jin, C. H.; Liang, X. L.; Chen, Q.; Peng, L. M. *Adv. Funct. Mater.* **2007**, *17*, 2478.
(25) Freeouf, J. L.; Woodall, J. M. *Appl. Phys. Lett.* **1981**, *39*, 727.
(26) Sze, S. M. *Physics of semiconductor devices, 281*; John Wiley & Sons: New York, 1981.
(27) Fan, Z. Y.; Lu, J. G. *Appl. Phys. Lett.* **2005**, *86*, 032111.
(28) Liu, Y.; Kauser, Z.; Ruden, P. P.; Hassan, Z.; Lee, Y. C.; Ng, S. S.; Yam, F. K. *Appl. Phys. Lett.* **2006**, *88*, 022109.
(29) Reference 28 shows that the strain/stress dependence of A** arises only from the stress/strain dependence of the effective mass. The ratio of change effect mass to change of band gaps with strain/stress is about 0.1%. Thus, the small change of A** is neglected. He and Yang's report in ref 15 indicated that large piezoresistance effect of silicon nanowire derives mainly from the change in mobility rather that carrier density, so N_D under various strain in our experiments can be considered as constant.
(30) Shan, W.; Li, M. F.; Yu, P. Y.; Hansen, W. L.; Walukiewicz, W. *Appl. Phys. Lett.* **1988**, *53*, 974.
(31) Chung, K. W.; Wang, Z.; Costa, J. C.; Williamson, F.; Ruden, P. P.; Nathan, M. I. *Appl. Phys. Lett.* **1991**, *59*, 1191.
(32) Liu, Y.; Kauser, M. Z.; Nathan, M. I.; Ruden, P. P.; Dogan, S.; Morkoc, H.; Park, S. S.; Lee, K. Y. *Appl. Phys. Lett.* **2004**, *84*, 2112.
(33) Dridi, Z.; Bouhafs, B.; Ruterana, P. *New J. Phys.* **2002**, *4*, 94.
(34) Li, Y. F.; Yao, B.; Lu, Y. M.; Cong, C. X.; Zhang, Z. Z.; Gai, Y. Q.; Zheng, C. J.; Li, B. H.; Wei, Z. P.; Shen, D. Z.; Fan, X. W.; Xiao, L.; Xu, S. C.; Liu, Y. *Appl. Phys. Lett.* **2007**, *91*, 021915.
(35) Cao, J.; Wang, Q.; Dai, H. *Phys. Rev. Lett.* **2003**, *90*, 157601.
(36) Liu, Y.; Kauser, M. Z.; Schroepfer, D. D.; Ruden, P. P.; Xie, J.; Moon, Y. T.; Onojima, N.; Morkoc, H.; Son, K. A.; Nathan, M. I. *J. Appl. Phys.* **2006**, *99*, 113706.

NL802367T